Supramolecular Chemistry Hot Paper

International Edition: DOI: 10.1002/anie.201804620
German Edition: DOI: 10.1002/ange.201804620

Photo-Controlled Reversible Microtubule Assembly Mediated by Paclitaxel-Modified Cyclodextrin

*Ying-Ming Zhang, Ni-Yuan Zhang, Kui Xiao, Qilin Yu, and Yu Liu**

Abstract: *The design and construction of multi-stimuli-responsive supramolecular nanoassemblies that can mimic and regulate the fundamental biological processes have become a focus of interest in supramolecular chemistry. In this work, a perfect combination has been achieved between naturally occurring microtubules and artificially macrocyclic receptors. The self-assembling morphology of microtubules can be photo-tuned by the host–guest interaction of paclitaxel-modified β-cyclodextrin (PTX-CD) and photochromic arylazopyrazole (PTX-AAP). Moreover, the supramolecularly aggregated microtubules in a cellular environment can induce a pronounced cell morphological change and cell death. This supramolecular approach based on the secondary PTX-AAP⊂PTX-CD complexation provides us a facile method to reversibly control the intertubular aggregation behaviors of microtubules, which may bring new perspectives in the treatment of diseases related to improper protein aggregation.*

Supramolecular chemistry, which is ubiquitously practiced in nature, has been proven as a powerful strategy in the formation of many highly ordered and functionalized biostructures (for example, cytoplasmic microtubules and viral capsids) by precisely controlling the noncovalent interactions.[1] Motivated by the wisdom of nature, artificially self-organized nanoarchitectures, particularly the ones based on macrocyclic receptors (for example, cyclodextrins, calixarenes, and cucurbiturils), have provided numerous structurally and kinetically well-defined model systems to simplify, mimic, or even regulate biological and physiological events.[2,3] Thus, control over the self-assembly of biological molecules with synthetic molecules is highly desirable and represents one of the increasingly significant topics in supramolecular chemistry.[4,5]

As one of the fundamental components in all eukaryotic cells, microtubules (MTs) are cytoskeletal polymers that are assembled from dynamically alternating α/β tubulin heterodimers and play a vital role in the mitosis-related cell cycle (Scheme 1 a).[6] Meanwhile, among the numerous macrocyclic molecules available for host–guest interactions, cyclodextrins (CDs) have been intensively studied and can be readily endowed with stimuli-responsiveness by direct chemical modification and intermolecular complexation with their intrinsic hydrophobic cavities.[7] In line with these fascinating features, one can believe that the synergetic integration of MTs and CDs into a single supramolecular assembled entity will eventually create more innovative biomaterials with structural and functional diversity.

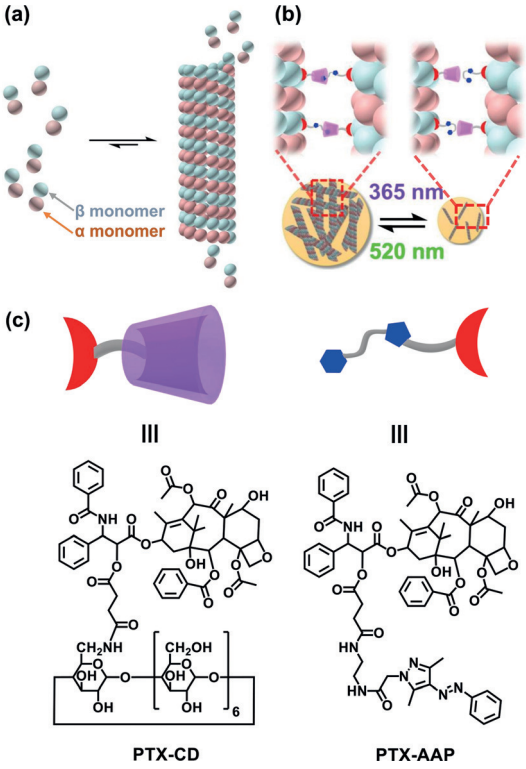

Scheme 1. Schematic and molecular structures of (PTX-AAP⊂PTX-CD)@MT ternary supramolecular assembly.

Herein, we demonstrate that the intertubular aggregation of MTs can be reversibly light-controlled by the incorporation of β-CD and photochromic arylazopyrazole (AAP). In our case, the interconnection with MTs was realized by the covalent modification of CD and AAP with paclitaxel (PTX), a clinically approved anticancer drug that can hyperstabilize MTs against depolymerization by selectively binding of each β-monomer (Scheme 1).[8] Spectroscopic and microscopic investigations jointly demonstrate that the induction of MT aggregation by supramolecular complexation can lead to

[*] Dr. Y.-M. Zhang, N.-Y. Zhang, K. Xiao, Dr. Q. Yu, Prof. Dr. Y. Liu
College of Chemistry, State Key Laboratory of Elemento-Organic Chemistry, Nankai University
Tianjin 300071 (China)
E-mail: yuliu@nankai.edu.cn
Prof. Dr. Y. Liu
Collaborative Innovation Center of Chemical Science and Engineering (Tianjin)
Tianjin 300072 (China)
Supporting information and the ORCID identification number(s) for the author(s) of this article can be found under: https://doi.org/10.1002/anie.201804620.

a broad range of morphological variation from nanofibers and nanoribbons to spherical nanoparticles with different sizes (Scheme 1 b). More significantly, the MT aggregation can be realized also in the cellular environment, ultimately leading to more serious cell morphological changes and cell death. To the best of our knowledge, synthetic macrocyclic motifs have not been applied thus far as inducers of photo-controlled MT aggregation.

The construction of (PTX-AAP⊂PTX-CD)@MT supramolecular assembly is depicted in Scheme 1. The host compound PTX-CD was synthesized by the amide condensation between 2′-succinyl PTX and mono-6-deoxy-6-amino-β-CD. Meanwhile, the skeleton of PTX was endowed with photochromic properties using amino-substituted AAP under similar reaction conditions. Superior to the conventional azobenzene, AAP derivatives exhibit strikingly distinctive binding affinities with β-CD in their reversible *E*(*trans*)/*Z*(*cis*) photoisomerization process.[9] The molecular structures and proton designations of PTX-AAP and PTX-CD were clearly characterized and assigned in the Supporting Information (Figures S1–S9). It is believed that the esterification and subsequent modification at 2′-*O*-position of PTX would not have a negative impact on the biological activity (Figure S10, Supporting Information).[10]

Next, the photoisomeric properties of PTX-AAP were investigated in the presence of native β-CD by UV/Vis spectroscopy. As discerned from Figure 1 a, PTX-AAP showed reversible photophysical behaviors; that is, upon UV irradiation at 365 nm, the π→π* transition ranging in 290–390 nm exhibited a significant decrease, and the maximum absorption peak was hypochromatically shifted from 330 nm to 288 nm. Meanwhile, the characteristic absorption of the n→π* band around 430 nm dramatically increased, accompanied by a slight bathochromic shift. Comparatively, upon visible light irradiation at 520 nm, the intensity of π→π* band was largely recovered, corresponding to the reverse *cis*- and *trans*-photoisomerization with a fairly high efficiency above 80%. It is also noteworthy that the cycle in the photoinduced isomerization of PTX-AAP could be repeated at least four times without any change in the UV/Vis spectra (Figure 1 a, inset). Undoubtedly, the excellent photoisomerization in PTX-AAP⊂β-CD system would facilitate the morphological transformation and biofunctional regulation of the (PTX-AAP⊂PTX-CD)@MT ternary supramolecular assembly at the cellular level, as described below.

Furthermore, the isomerization of PTX-AAP from *trans*- to *cis*-configuration was quantitatively determined by ^{1}H NMR spectroscopy. In this case, sufficient light irradiation was implemented to ensure the complete photochromic transformation between $PSS_{E\rightarrow Z}$-PTX-AAP and $PSS_{Z\rightarrow E}$-PTX-AAP (Figure 1 b). As compared to the *E*-PTX-AAP, it is found that the resonance signals of phenyl and amide protons in $PSS_{E\rightarrow Z}$-PTX-AAP, especially the ones close to the azobenzene center (H_1), underwent a pronounced upfield shift as a result of the photoswitchable isomerization from *trans*- to *cis*-isomer after UV irradiation at 365 nm. Moreover, the chemical shifts of these characteristic protons were almost recovered to the original state upon subsequent irradiation at 520 nm. The singlet resonance peak at 6.3 ppm assigned to the

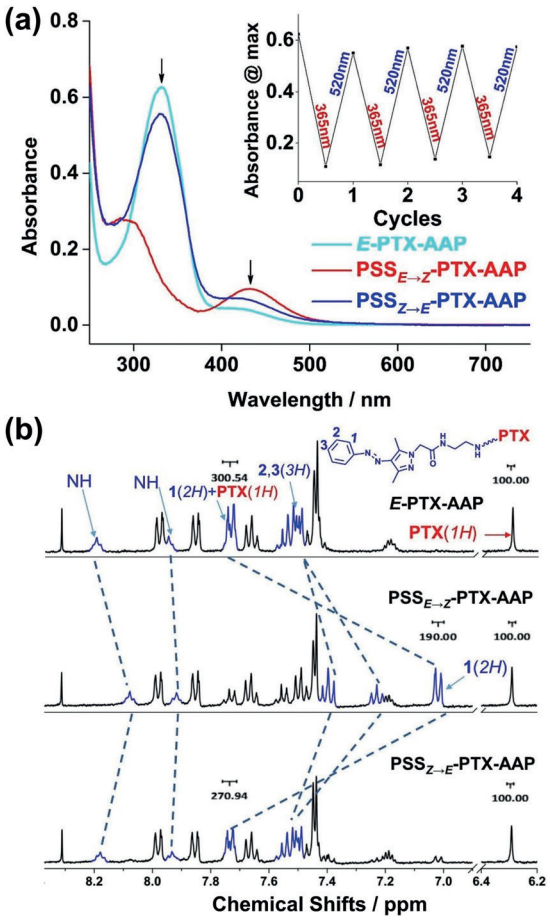

Figure 1. a) UV/Vis spectra of the photoisomerization of PTX-AAP⊂β-CD complex in water at 25 °C ([PTX-AAP] = 50 μM and [β-CD] = 500 μM). Inset: UV/Vis absorption intensity changes at 330 nm observed upon alternating UV (365 nm) and visible-light (520 nm) irradiation. b) ^{1}H NMR spectra of *E*-PTX-AAP before and after UV irradiation at 365 nm for 60 min, and then exposed to visible-light irradiation at 520 nm for another 30 min in [D_6]DMSO at 25 °C. PSS = photostationary state.

10-H position of PTX was chosen as the internal standard to clearly verify the photo-transformation efficiency. Thus, based on the integral ratio changes of aromatic proton (H_1) before and after light irradiation, the conversion efficiency in PTX-AAP could be calculated as 95% and 85% for $E\rightarrow Z$ and $Z\rightarrow E$ photoisomerization, respectively, which are in good agreement with the UV/Vis spectroscopic results.

After validating the photoisomerization of PTX-AAP, the noncovalent cross-linkage and the subsequent morphological conversion of MTs induced by the PTX-AAP⊂PTX-CD complex were investigated by transmission electron microscopy (TEM). As shown in Figure 2, diverse morphologies could be observed when tubulins were co-incubated with different PTX-containing compounds. Initially, the pristine tubulin could be spontaneously reconstituted into uniform MTs and presented as one-dimensional nanofibers with length of several micrometers, reflecting a dynamic equilibrium with monomeric tubulins in general tubulin buffer solution (Figure 2 a).[11] Then, the addition of equimolar PTX could apparently enhance the polymerization process of MTs,

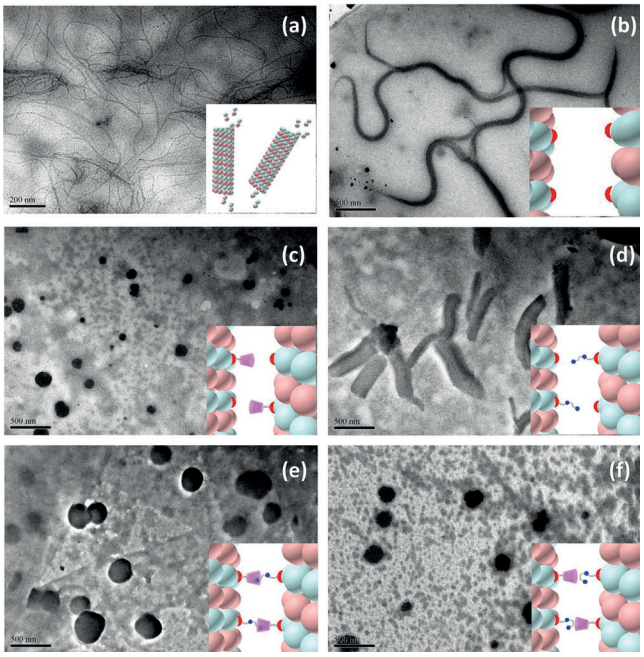

Figure 2. TEM images of a) free MTs (scale bar = 200 nm) and MTs with b) PTX c) PTX and PTX-CD, d) PTX and *trans*-PTX-AAP, e) *trans*-PTX-AAP and PTX-CD, and f) *cis*-PTX-AAP and PTX-CD. [tubulin] = 1 mg mL^{-1}, [PTX] = 4.5 μM, [PTX-CD] = 4.5 μM, [PTX-AAP] = 4.5 μM, scale bar = 500 nm in (b–f).

and the diameters of the obtained nanotubes dramatically increased from 25 nm to 60 nm with PTX, which is mainly attributed to the stabilization effect of PTX upon binding to the more dynamic β-monomer end of MTs (Figure 2b).[8] Moreover, the aggregation of free PTX and PTX-CD with fibrous MTs was converted to small spherical nanoparticles, 117 nm in diameter, probably owing to the fairly weak intermolecular complexation between free PTX skeleton and β-CD's cavity (Figure 2c).[12] In addition, thin nanoribbons were observed upon mixing with PTX-AAP, indicating that the introduction of hydrophobic PTX-AAP could drastically affect the arrangement of α/β dimeric subunits in MTs (Figure 2d). Interestingly, large nanoparticulate aggregates with an average size of 286 nm were exclusively formed through the multivalent cross-linkage of the PTX-AAP⊂PTX-CD complex (Figure 2e).[13] More significantly, once *trans*-PTX-AAP was transformed into the *cis*-isomer under UV irradiation, the bulky *cis* form was expelled from the cavity of β-CD, thus leading to the recovery of small nanospheres, 175 nm in diameter, in the dried state (Figure 2f).[14] This result is consistent with that of MTs with PTX and PTX-CD, implying that no obvious host–guest complexation occurred in the β-CD-pendant MTs (Figure 2c,f).

Along with the microscopy results, the photo-controlled multivalent binding of MT with PTX-AAP and PTX-CD was further confirmed by the dynamic light scattering and UV transmittance studies. As expected, the size distribution was obviously changed in aqueous solution; that is, the tubulin with PTX/PTX-CD or PTX/PTX-AAP in buffer solution showed a narrow size distribution, whereas it was drastically broadened in the case of the PTX-AAP⊂PTX-CD complex and the solution instantly turned turbid, indicative of the formation of large aggregates through host–guest complexation. In comparison, after irradiation at 365 nm for 15 min, the narrow size distribution was recovered, corresponding to the dissipation of cross-linked supramolecular aggregates (Figure S11, Supporting Information). Moreover, the optical transmittance of MT alone was nearly 100% in the long-wavelength region and only a slight decrease was observed for individual PTX, PTX-CD, and PTX-AAP, again corroborating the enhancement effect of PTX in the tubulin polymerization process. Remarkably, the transmittance of MTs sharply decreased with the *trans*-PTX-AAP⊂PTX-CD complex as cross-linker. Owing to the superior photochromic characteristics of PTX-AAP, the transmittance was recovered to the original level under UV irradiation (Figure 3). In the control experiments, no decline in transmittance could be

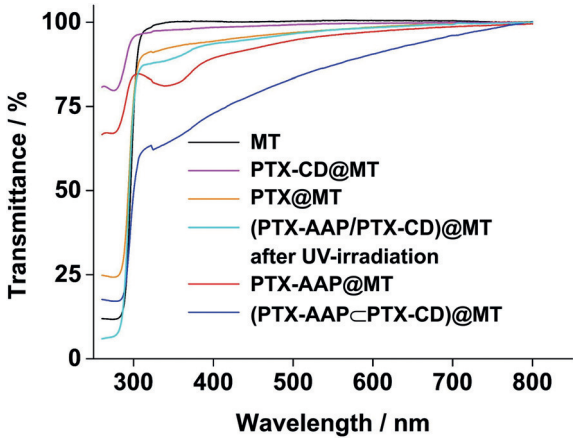

Figure 3. Optical transmittance of tubulin (0.044 mg mL^{-1}) with free PTX (0.4 μM) PTX-CD (0.4 μM), PTX-AAP (0.4 μM), and their corresponding binary complex ([PTX-CD] = [PTX-AAP] = 0.2 μM) in general tubulin buffer solution (pH 6.8) at 25 °C.

observed without tubulin (Figure S12, Supporting Information). These results jointly demonstrate that the monovalent association between PTX-AAP and PTX-CD is not sufficient to form large assemblies and the multiply cooperative interaction mediated by PTX-AAP⊂PTX-CD inclusion complexation is indispensable to induce the intertubular aggregation of MTs in solution.

Furthermore, the fluorescence-dye-staining assays were exploited to study the complexation-induced intertubular aggregation at the cellular level (Figure 4a). Initially, the normal MTs labeled by fluorescein isothiocyanate (FITC)-tagged antibody were uniformly distributed in the whole A549 cell (the human lung tumor cell line). Moreover, no obvious aggregation was observed in these cells when treated with the individual host or guest compound, but there was a slight tendency for MTs to aggregate in the case of *trans*-PTX-AAP. In keen contrast, nanoparticulate aggregates with diameter of approximately 4–8 μm were found around cell nuclei in the *trans*-PTX-AAP⊂PTX-CD complex group, accompanied by the irregular change in cell morphology. Comparatively, the morphological characteristics of the selected cell line turned to the normal stage and the micro-

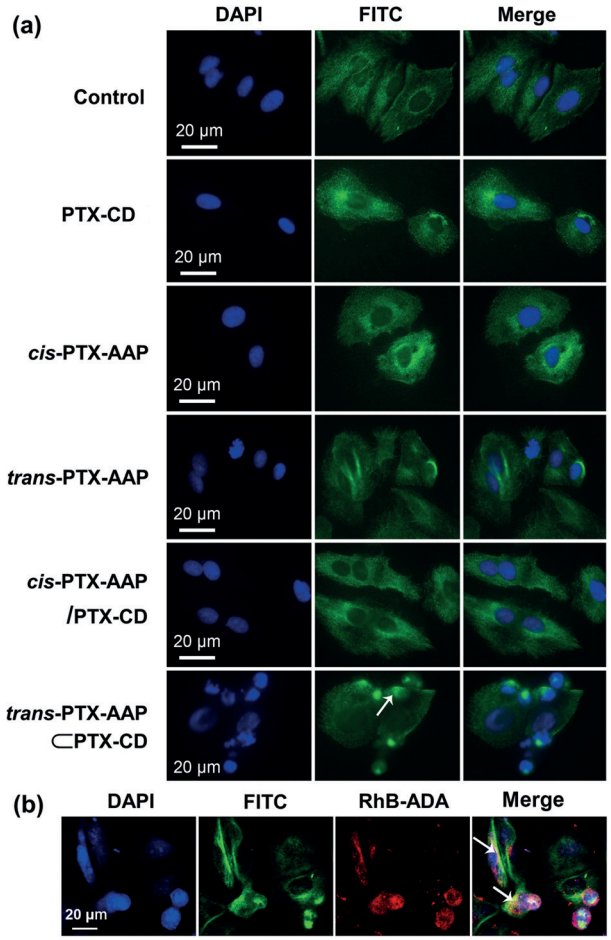

Figure 4. Confocal microscopy images of a) A549 cell line after treatment with PTX-CD, PTX-AAP, and their corresponding complexes; b) co-localization of aggregated MTs and *trans*-PTX-AAP⊂PTX-CD complex. 4′,6-Diamidino-2-phenylindole dihydrochloride hydrate (DAPI) was used to stain the nucleus. The typical compact MTs are indicated by white arrows.

tubular aggregation could be largely eliminated in *cis*-PTX-AAP/PTX-CD group. Moreover, the number of cells possessing condensed MTs was counted, which is fully consistent with the results obtained from the confocal microscopy experiments (Figure S13, Supporting Information). Meanwhile, adamantane-bearing rhodamine B (RhB-ADA) was used to further co-localize the compact MTs induced by the PTX-AAP⊂PTX-CD complex because of the much higher binding strength between β-CD and ADA. Indeed, both the linear and spherical aggregated MTs were concurrently labeled by FITC and RhB, further confirming the supramolecular inductive effect in cells (Figure 4b).

Finally, propidium iodide (PI) staining experiments were performed to investigate the influence of intertubular aggregation on the cell viability. Among all the examined groups, the extensive host–guest interaction between *trans*-PTX-AAP and PTX-CD caused relatively higher cell death (12.0%), while this value stayed at only 7.8% when treated by *cis*-PTX-AAP and PTX-CD. It is also noteworthy that the cell death was largely inhibited once the compact MTs were disassembled by the addition of native β-CD as a competitive host (6.7%). In addition, more shrunken cells were found after treatment with the binary complex and thus this cell death is associated with cell shrinkage, an effect most likely resulting from the intracellular aggregation of supramolecularly cross-linked MTs (Figure S14, Supporting Information).

In conclusion, the present studies show that benefitting from both the stabilization of PTX in MTs and the reversible photoisomerization of PTX-AAP with PTX-CD, the intertubular aggregation behavior of MTs could be efficiently regulated under light irradiation with different wavelengths. Moreover, as investigated by the cell-staining experiments, the intertubular aggregation of MTs induced by PTX-AAP⊂PTX-CD complexation exhibited a dramatic cell morphological change and a relatively higher cytotoxic effect. Thus, we can envision that future research on the synergetic combination of natural MTs and artificial stimuli-switchable components as building blocks will allow us not only to promote our molecular-level understanding of the spontaneous and dynamic protein nanoassemblies but also to open bright prospects in MT aggregation-related disease diagnosis and treatment.

Acknowledgements

This work was financially supported by the National Natural Science Foundation of China (grants 21432004, 21472100, 21772099, and 91527301).

Conflict of interest

The authors declare no conflict of interest.

Keywords: cyclodextrin · microtubules · molecular recognition · photo-responsiveness · supramolecular assembly

How to cite: *Angew. Chem. Int. Ed.* **2018**, *57*, 8649–8653
Angew. Chem. **2018**, *130*, 8785–8789

[1] a) Q. Luo, C. Hou, Y. Bai, R. Wang, J. Liu, *Chem. Rev.* **2016**, *116*, 13571–13632; b) L.-G. Milroy, T. N. Grossmann, S. Hennig, L. Brunsveld, C. Ottmann, *Chem. Rev.* **2014**, *114*, 4695–4748; c) M. Guix, C. C. Mayorga-Martinez, A. Merkoçi, *Chem. Rev.* **2014**, *114*, 6285–6322.

[2] a) D.-H. Qu, Q.-C. Wang, Q.-W. Zhang, X. Ma, H. Tian, *Chem. Rev.* **2015**, *115*, 7543–7588; b) K. I. Assaf, W. M. Nau, *Chem. Soc. Rev.* **2015**, *44*, 394–418; c) S. J. Barrow, S. Kasera, M. J. Rowland, J. del Barrio, O. A. Scherman, *Chem. Rev.* **2015**, *115*, 12320–12406; d) X. Ma, Y. Zhao, *Chem. Rev.* **2015**, *115*, 7794–7839; e) X.-Y. Hu, T. Xiao, C. Lin, F. Huang, L. Wang, *Acc. Chem. Res.* **2014**, *47*, 2041–2051; f) A. R. Urbach, V. Ramalingam, *Isr. J. Chem.* **2011**, *51*, 664–678; g) M.-M. Russew, S. Hecht, *Adv. Mater.* **2010**, *22*, 3348–3360.

[3] a) S. Engel, N. Möller, B. J. Ravoo, *Chem. Eur. J.* **2018**, *24*, 4741–4748; b) A. M. Doolan, M. L. Rennie, P. B. Crowley, *Chem. Eur. J.* **2018**, *24*, 984–991; c) R. Mejia-Ariza, L. Graña-Suárez, W. Verboom, J. Huskens, *J. Mater. Chem. B* **2017**, *5*, 36–52; d) M. L. Rennie, A. M. Doolan, C. L. Raston, P. B. Crowley, *Angew. Chem. Int. Ed.* **2017**, *56*, 5517–5521; *Angew. Chem.* **2017**, *129*, 5609–5613; e) R. E. McGovern, S. C. Feifel, F. Lisdat, P. B. Crowley, *Angew. Chem. Int. Ed.* **2015**, *54*, 6356–6359; *Angew.*

Chem. **2015**, *127*, 6454 – 6457; f) Á. Martínez, C. Ortiz Mellet, J. M. García Fernández, *Chem. Soc. Rev.* **2013**, *42*, 4746 – 4773; g) G. Chen, M, Jiang, *Chem. Soc. Rev.* **2011**, *40*, 2254 – 2266.

[4] a) S. van Dun, C. Ottmann, L.-G. Milroy, L. Brunsveld, *J. Am. Chem. Soc.* **2017**, *139*, 13960 – 13968; b) K. Petkau-Milroy, L. Brunsveld, *Org. Biomol. Chem.* **2013**, *11*, 219 – 232.

[5] a) P. J. de Vink, J. M. Briels, T. Schrader, L.-G. Milroy, L. Brunsveld, C. Ottmann, *Angew. Chem. Int. Ed.* **2017**, *56*, 8998 – 9002; *Angew. Chem.* **2017**, *129*, 9126 – 9130; b) S.-R. Wang, Y.-Y. Song, L. Wei, C.-X. Liu, B.-S. Fu, J.-Q. Wang, X.-R. Yang, Y.-N. Liu, S.-M. Liu, T. Tian, X. Zhou, *J. Am. Chem. Soc.* **2017**, *139*, 16903 – 16912; c) Y.-M. Zhang, X.-J. Zhang, X. Xu, X.-N. Fu, H.-B. Hou, Y. Liu, *J. Phys. Chem. B* **2016**, *120*, 3932 – 3940; d) S. Biswas, K. Kinbara, T. Niwa, H. Taguchi, N. Ishii, S. Watanabe, K. Miyata, K. Kataoka, T. Aida, *Nat. Chem.* **2013**, *5*, 613 – 620; e) J. M. Chinai, A. B. Taylor, L. M. Ryno, N. D. Hargreaves, C. A. Morris, P. J. Hart, A. R. Urbach, *J. Am. Chem. Soc.* **2011**, *133*, 8810 – 8813; f) L. Zhang, Y. Wu, L. Brunsveld, *Angew. Chem. Int. Ed.* **2007**, *46*, 1798 – 1802; *Angew. Chem.* **2007**, *119*, 1830 – 1834.

[6] a) A. Akhmanova, M. O. Steinmetz, *Nat. Rev. Mol. Cell Biol.* **2015**, *16*, 711 – 726; b) K. C. Nicolaou, F. Roschangar, D. Vourloumis, *Angew. Chem. Int. Ed.* **1998**, *37*, 2014 – 2045; *Angew. Chem.* **1998**, *110*, 2120 – 2153.

[7] a) Y. Chen, Y. Liu, *Adv. Mater.* **2015**, *27*, 5403 – 5409; b) C. Yang, Y. Inoue, *Chem. Soc. Rev.* **2014**, *43*, 4123 – 4143.

[8] H. Xiao, P. Verdier-Pinard, N. Fernandez-Fuentes, B. Burd, R. Angeletti, A. Fiser, S. B. Horwitz, G. A. Orr, *Proc. Natl. Acad. Sci. USA* **2006**, *103*, 10166 – 10173.

[9] a) M. Wiemann, R. Niebuhr, A. Juan, E. Cavatorta, B. J. Ravoo, P. Jonkheijm, *Chem. Eur. J.* **2018**, *24*, 813 – 817; b) L. Stricker, E.-C. Fritz, M. Peterlechner, N. L. Doltsinis, B. J. Ravoo, *J. Am. Chem. Soc.* **2016**, *138*, 4547 – 4554.

[10] J. Li, Y. Gao, Y. Kuang, J. Shi, X. Du, J. Zhou, H. Wang, Z. Yang, B. Xu, *J. Am. Chem. Soc.* **2013**, *135*, 9907 – 9914.

[11] E. N. Cline, M.-H. Li, S. K. Choi, J. F. Herbstman, N. Kaul, E. Meyhöfer, G. Skiniotis, J. R. Baker, R. G. Larson, N. G. Walter, *Biomacromolecules* **2013**, *14*, 654 – 664.

[12] Y. Liu, G.-S. Chen, L. Li, H.-Y. Zhang, D.-X. Cao, Y.-J. Yuan, *J. Med. Chem.* **2003**, *46*, 4634 – 4637.

[13] a) C. Fasting, C. A. Schalley, M. Weber, O. Seitz, S. Hecht, B. Koksch, J. Dernedde, C. Graf, E.-W. Knapp, R. Haag, *Angew. Chem. Int. Ed.* **2012**, *51*, 10472 – 10498; *Angew. Chem.* **2012**, *124*, 10622 – 10650; b) J. Huskens, *Curr. Opin. Chem. Biol.* **2006**, *10*, 537 – 543.

[14] Z.-Q. Li, Y.-M. Zhang, H.-Z. Chen, J. Zhao, Y. Liu, *J. Org. Chem.* **2013**, *78*, 5110 – 5114.

Manuscript received: April 20, 2018
Accepted manuscript online: May 20, 2018
Version of record online: June 21, 2018

